

A continuous-variable quantum repeater with quantum scissors

Kaushik P. Seshadreesan¹, Hari Krovi², and Saikat Guha¹

¹*College of Optical Sciences, University of Arizona, Tucson, AZ 85721, USA*

²*Quantum Engineering and Computing Physical Sciences and Systems,
Raytheon BBN Technologies, Cambridge, MA 02138, USA*

(Dated: December 15, 2024)

We present a continuous-variable quantum repeater scheme for entanglement distribution over a lossy bosonic channel using two-mode squeezed vacuum state sources. The scheme uses the quantum scissors operation for entanglement distillation. Rates per use of the channel achieved by the scheme are boosted by a layer of switched channel multiplexing. By suitably choosing the entanglement source and distillation parameters, degree of channel multiplexing and number of repeater nodes, the scheme is shown to beat the direct transmission exponential rate-loss trade-off.

A *quantum internet* [1] that distributes entanglement and quantum-secure shared secret key at high rates over large distances exemplifies the goal of quantum communications [2]. It would enable, e.g., unconditionally secure multiparty classical communications [3], distributed quantum computation, sensing, and other quantum information processing applications [4–9]. The main hurdle in the way of establishing the quantum internet is photon loss. Entanglement distribution rates over a lossy bosonic channel such as an optical fiber or free space link are known to drop exponentially with loss [10]. The entanglement distribution capacity of the lossy bosonic channel of transmissivity η under unlimited two-way local operations and classical communication (LOCC) assistance was recently established to be $C_{\text{direct}} = -\log_2(1 - \eta)$ entangled qubit pairs per channel-use [11, 12] (see also [13] for a strong converse theorem).

Quantum repeater nodes [14, 15] comprised of entanglement sources, distillation schemes and memories when interspersed over the channel can circumvent this exponential rate-loss tradeoff. For discrete-variable (DV) quantum states of single photon polarization or time-bin degrees of freedom, repeater schemes [16, 17] based on matter memories [18] as well as optical memories [19, 20] have been developed. Alternatively, quantum information can also be encoded in the continuous quadratures of the electromagnetic field modes, also known as quantum continuous variables (CV). Since CV quantum states can be generated using coherent lasers, they allow for easier integration with classical telecommunications. However, quantum repeaters for CV remain to be well established.

It is known that Gaussian quantum operations, namely physical operations that map Gaussian states to other Gaussian states, alone cannot act as quantum repeaters for CV [21, 22]. Ralph proposed a scheme based on heralded non-deterministic noiseless linear amplification (NLA) [23] that performs error correction [24] against the Gaussian noise arising from the action of a pure loss channel on one mode of a two-mode squeezed vacuum (TMSV) entangled state. Using the non-Gaussian quantum scissors operation [23, 25] which approximates NLA for low mean photon number states, Dias and

Ralph [26, 27] showed that the entangled state heralded by the successful operation of a single quantum scissors across the lossy channel is more entangled than the corresponding plain lossy TMSV state in terms of the logarithmic negativity [28, 29] and entanglement of formation [30] measures. The present authors [31] evaluated the reverse coherent information (RCI) [11, 32–35] of the state heralded by NLA with multiple quantum scissors, which is a lower bound on its distillable entanglement, where the latter operationally quantifies the number of ebits that can be distilled from an asymptotically large number of copies of the heralded state using LOCC. It was shown that the heralded RCI can exceed $C_{\text{direct}}(\eta)$ —a necessary condition for a distillation scheme to be useful in a repeater scheme. The CV error correction scheme of [24] was recently generalized to the thermal loss channel [36]. NLA, both ideal [37], and approximate, based on quantum scissors [38], was shown to increase the range of CV quantum key distribution (QKD) in the presence of thermal noise.

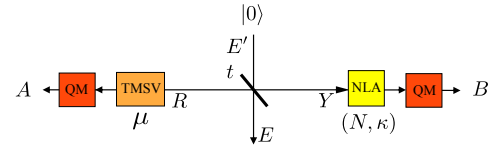


Figure 1. A repeater link for CV quantum communication consisting of a two-mode squeezed vacuum (TMSV) state source, N -quantum scissors NLA, and quantum memory QM. For a chain of n repeater links over a channel of transmissivity η , the single link transmissivity is $t = \eta^{1/n}$.

In this letter, using repeater nodes consisting of TMSV sources for entanglement generation, the quantum scissors for entanglement distillation (Fig. 1), a non-Gaussian entanglement swap operation [39] to connect adjacent repeater links (segmented portions of the lossy channel arising from introducing repeater nodes), and a layer of switched channel multiplexing across each repeater link to boost the end-to-end per-channel-use rates, we present a CV quantum repeater scheme (Fig. 2) that outperforms $C_{\text{direct}}(\eta)$. The main findings and contri-

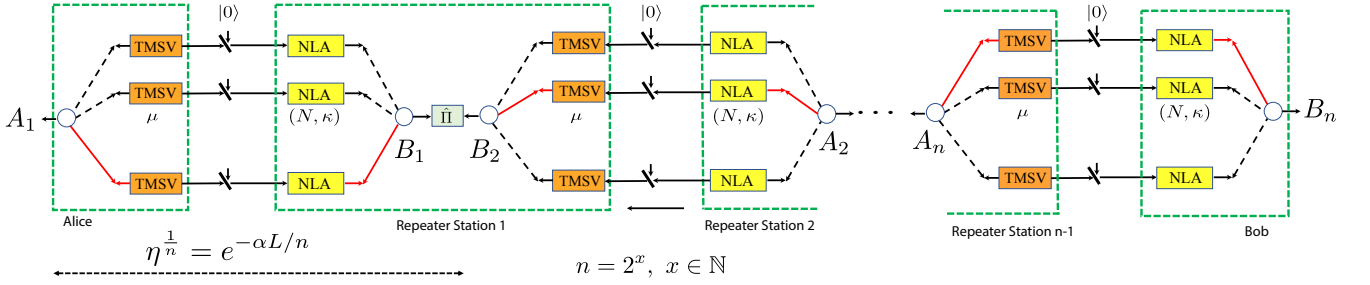


Figure 2. A CV quantum repeater scheme based on the repeater links of Fig. 1 and switched channel multiplexing. The operator $\hat{\Pi}$ refers to a non-Gaussian entangled state projection as described in (2). The empty circles denote switches. Quantum memories are suppressed for brevity.

contributions behind the working of the scheme include the following: i) It is optimal to use NLA based on a single quantum scissors for entanglement distillation in CV quantum repeaters compared to any higher number of scissors. This is because the product of the heralded RCI and the heralding success probability, numerically optimized over the free parameters of the system, is maximal for the single quantum scissors. ii) The optimal heralded RCI with a single quantum scissors in a repeater link of transmissivity t approaches 1 independently of the channel transmissivity t , which implies that the optimal heralded state approaches a perfect ebit (Note that the RCI of an ebit by definition is one); the corresponding success probability is found to scale proportional to t when $t \ll 1$. The limiting case is clearly unphysical, since it would require quantum scissors of infinite NLA gain. Yet, it carries semblance to DV repeaters, where entanglement distillation is typically based on the successful detection of photons arriving at a repeater node, such that a successful detection event heralds a perfect ebit of entanglement and the detection success probability scales proportional the transmissivity of the repeater link. This prompts us to consider switched channel multiplexing across each repeater link similarly to the DV case [17] as a way to boost the end-to-end rates. iii) The DV-like mode of operation of CV repeater links of Fig. 1 is far from optimal. We derive an explicit iterative analytic formula for the end-to-end entangled quantum state heralded across the CV repeater chain in Fig. 2 for different number of repeater nodes. We identify a mode of operation in terms of the parameters involved wherein the individual CV repeater link states are far from being perfect ebits, but the success probability is higher compared to the DV-like mode of operation, resulting in a superior overall end-to-end entanglement distribution rate-distance tradeoff compared to the DV-like mode of operation, thus revealing the full potential of the CV repeater scheme.

Note that, prior to this work, Furrer and Munro have proposed a CV repeater scheme based on alternative non-Gaussian entanglement distillation schemes—symmetric

photon replacement and purifying distillation [40, 41], that beats $C_{\text{direct}}(\eta)$ [39]. Their scheme involves iterative use of entanglement distillation, which necessitates classical communication between repeater nodes beyond nearest neighbors, whereas ours only requires nearest neighbor classical communications. Also, the quantum scissors involves fewer DV resources (single photon injection and detection) compared to the non-Gaussian distillation schemes considered in [39], making it simpler to implement. Further, while the analysis presented in [39] considers a Gaussified version of the end-to-end heralded non-Gaussian state, our analysis is based on the exact non-Gaussian state heralded across the repeater chain.

CV repeater link based on the quantum scissors: Consider a repeater link of transmissivity t , with a TMSV entangled source of mean photon number μ and approximate NLA of gain $g = \sqrt{(1-\kappa)/\kappa}$ implemented by N -quantum scissors at the output of the channel (where κ is an intrinsic parameter of the scissors), as depicted in Fig. 1. For $N > 1$, the quantum scissors-based NLA module does the following (c.f. [31, Fig. 1]): i) Splits the signal quantum state into N equal parts. ii) Each sub-signal undergoes the quantum scissors operation described in [25, 42], which involves linear optics, single photon injection and detection, and as the name suggests truncates the sub-signal quantum state in Fock space to its support on the subspace spanned by the 0 and 1 photon Fock states. (See [43–46] for a related notion of quantum scissors involving nonlinear optical elements). iii) Recombines the "chopped" subsignals into one mode. When the NLA succeeds, it heralds a noiselessly amplified [47] version of the signal state that is truncated to its support on the N -photon subspace spanned by $0, 1, \dots, N$ Fock states. Section I of the Supplemental Material describes the state heralded across the CV repeater link consisting of N -quantum scissors of Fig. 1 in the Fock basis, the associated heralding success probability, and an expression for the RCI of the state.

We numerically optimized the *true* RCI of the repeater link state, namely the product of the heralded RCI and the heralding success probability, over the TMSV mean

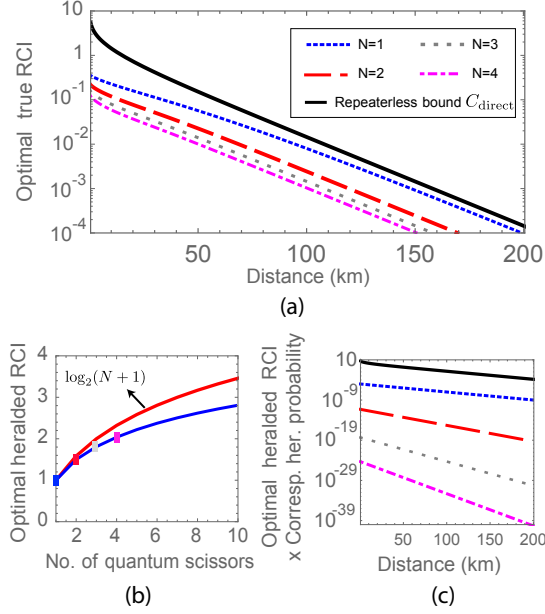


Figure 3. (a) The optimal true RCI of the repeater link state. (b) The optimal heralded RCI and (c) the corresponding heralding success probability (scaled by the former).

photon number and the gain of the quantum scissors, for different number of quantum scissors. The results are plotted in Fig. 3 (a). Firstly, all the curves lie below $C_{\text{direct}}(t)$, as should be the case by the very definition of the capacity. Secondly, the optimal true RCI is the highest for the single quantum scissors, which suggests its optimality compared to higher number of scissors.

Further, the RCI heralded by $N = 1, 2, 3, 4$ quantum scissors by itself is numerically optimized over the same set of parameters, and plotted in Figure 3 (b) as a function of N . The optimal heralded RCI in each case is found to approach a limiting constant independent of the channel transmissivity t . The constant for a single quantum scissors is found to be $\log_2(2) = 1$, which corresponds to a perfect ebit of entanglement. For $N > 1$, the constant is found to be less than $\log_2(N + 1)$, where $N + 1$ is the dimensionality of the output Hilbert space, which indicates that the optimal heralded entangled states do not approach perfect “e-dits” except when $N = 1$. In Fig. 3 (c), the asymptotic scaling ($t \ll 1$) of the heralding success probability corresponding to the optimal RCI (scaled by the former) is plotted as a function of the transmission distance for different N and found to be $\propto t^N$.

Non-Gaussian entanglement swapping: Consider that the state heralded across a repeater link of Fig. 1 can be expressed as [48]

$$|\psi\rangle_{ABL} \propto (1 + \xi a^\dagger b^\dagger) \sigma_{AL}^\rho |0\rangle_{ABL} \quad (1)$$

where \hat{a} , \hat{b} are the repeater link mode operators, L is the loss mode, ξ a function of μ , κ , t , and σ_{AL}^ρ is the

two-mode squeezing operator corresponding to squeezing of magnitude ρ in modes A , L , where $\tanh \rho = \sqrt{1 - t} \tanh(\sinh^{-1} \sqrt{\mu})$, [49]. Clearly the state in (1) is non-Gaussian. In the limit of low TMSV mean photon number, to first approximation, the state in modes A , B is a pure state of the form

$$|\psi\rangle_{A_1 B_1} = (|0\rangle_{A_1} |0\rangle_{B_1} + \xi |1\rangle_{A_1} |1\rangle_{B_1}) / \sqrt{1 + \xi^2}. \quad (2)$$

At a repeater node, the entanglement in two such repeater link states $|\psi\rangle_{A_1 B_1}$ and $|\psi\rangle_{A_2 B_2}$ can thus be swapped by a non-Gaussian entangled projection operator of the form $\hat{\Pi} = |\phi\rangle\langle\phi|_{B_1 A_2}$, where $|\phi\rangle_{B_1 A_2} = (|0\rangle_{B_1} |0\rangle_{A_2} + q |1\rangle_{B_1} |1\rangle_{A_2}) / \sqrt{1 + q^2}$, with $q = 1/\xi$. Such a projection can be implemented by Fock state filtering [39, 40] and a sequence of displacement operations, photon subtraction and vacuum projection [39] [50].

Quantum Repeater based on switched channel multiplexing: In order to describe the idea behind switched channel multiplexing, let us for the moment consider a single-photon-based DV quantum repeater chain of $n = 2^x$, $x \in \mathbb{N}$ links of the type shown in Fig. 2, so that $t = \eta^{1/n}$. The DV source generates a perfect maximally entangled qubit pair (Bell pair), of which one of the qubits is transmitted through the lossy channel segment. Heralding the arrival of this transmitted photon after loss here signifies the distillation a perfect ebit (RCI $I_R=1$), which happens with a probability $p \propto t = c\eta^{1/n}$. Further, at each repeater node, one local photon and one photon received through the channel are combined on a Bell-basis entangling measurement. The measurement succeeds with a probability p_{swap} , accomplishing entanglement swapping across the repeater node.

By introducing a layer of switched multiplexing across each repeater link, e.g., using a large number of spectral modes from the source, the success probability p can be boosted. For M parallel channels in a repeater link, the probability that at least one of them succeeds in distilling an ebit of entanglement is given by

$$p_M = 1 - (1 - c\eta^{1/n})^M. \quad (3)$$

For the n -repeater link chain, where each link is M -multiplexed, the rate at which an ebit of entanglement can be distributed between the end nodes equals the probability that at least one of the M modes succeeds in each of the n links and the entanglement swaps at each of the $n - 1$ repeater nodes succeeds. It is given by the rate R (in units of ebits/c.u.) that obeys

$$M \times R = p_M^n p_{\text{swap}}^{n-1} \leq \begin{cases} p_{\text{swap}}^{n-1} \\ (Mc)^n \eta p_{\text{swap}}^{n-1} \end{cases} \quad (4)$$

From the first upper bound in (4), we have $n = \log(M \times p_{\text{swap}} \times R_{\text{UB}}) / \log p_{\text{swap}}$. The two upper

bounds intersect at $\eta = 1/(Mc)^n$. From the intersection, we have $n = -\log \eta / \log(Mc)$. Combining the two, we have

$$\log(M \times p_{\text{swap}} \times R_{\text{UB}}) = \left(\frac{\log(1/p_{\text{swap}})}{\log(Mc)} \right) \log \eta \quad (5)$$

$$\Rightarrow R_{\text{UB}} = \frac{1}{M \times p_{\text{swap}}} \eta^\tau, \quad \tau = \frac{\log(1/p_{\text{swap}})}{\log(Mc)}. \quad (6)$$

For $M > 1/(p_{\text{swap}}c)$, $\tau < 1$, which beats the direct transmission capacity $C_{\text{direct}} = -\log(1-\eta)$ when $\eta \ll 1$ since the latter becomes $\approx 1.44\eta$ in the limit. The R_{UB} represents an upper bound on the envelope of achievable rates with the repeater scheme. The exact envelope of achievable rates with the repeater scheme was shown to be [17]

$$R = \frac{1}{M \times p_{\text{swap}}} \eta^s, \quad s = \frac{\log(p_{\text{swap}}(1 - (1 - cz)^M))}{\log z}, \quad (7)$$

where z is the unique solution of the transcendental equation

$$\begin{aligned} (1 - (1 - cz)^M) \log(p_{\text{swap}}(1 - (1 - cz)^M)) \\ = cMz \log z (1 - cz)^{M-1}. \end{aligned} \quad (8)$$

DV-like operation of multiplexed CV repeater:

We now go back to the CV repeater link of Fig. 1 with a single quantum scissors. By operating the scissors such that the heralded state is a near-perfect ebit and the heralding success probability is $\propto t$ (the proportionality constant being $c = 5 \times 10^{-6}$ in the limit $t \ll 1$), along with the non-Gaussian Bell swap operation, we apply the switched channel multiplexed repeater chain rate formula of (7) to the repeater scheme in Fig. 2. Considering the numerically optimized value of $p_{\text{swap}} = 0.00463$ [51] for the near-perfect ebit CV repeater link states, it turns out that the degree of multiplexing M has to be at least of the order of 10^9 so that the envelope of repeater-enhanced rates (per channel use) scales as η^s with $s < 1$ in the high loss regime. Figure 4 shows the rate envelope plots for different M , where each of the plots is obtained by varying the number of repeaters in the multiplexed repeater chain. The rates are expressed in units ebits per channel use (ebits/c.u.). The channel is assumed to be an optical fiber with attenuation constant 0.2 dB/km loss. With $M \approx 10^9$, the scheme attains a rate that scales as η^s , where $s = 0.68$, which is found to beat the direct transmission rate at ≈ 1070 km transmission distance. Likewise, with $M \approx 10^{13}$, the scheme attains a rate exponent $s = 0.32$, beating the tradeoff at ≈ 800 km.

General operation of multiplexed CV repeater:

The simplicity of the above calculation of repeater performance is a consequence of choosing the idealized, DV-like mode of operation for the CV repeater links. However, this mode of operation is not necessarily optimal.

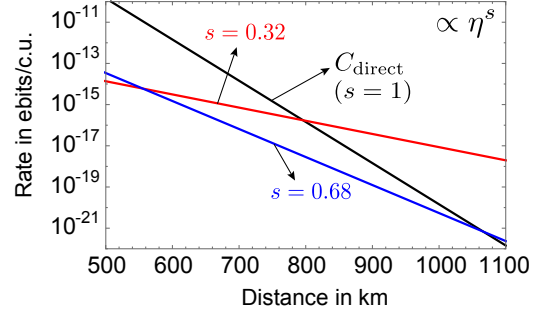


Figure 4. Envelope of achievable entanglement distribution rates obtained by varying the number of repeater nodes for the DV-like operation of the multiplexed CV repeater scheme. The different s parameter plots correspond to different degrees of multiplexing.

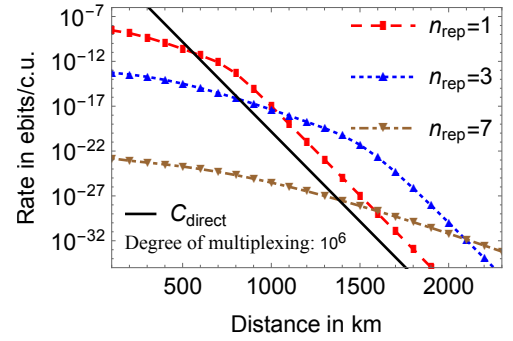


Figure 5. Entanglement distribution rates achieved by the multiplexed CV repeater scheme calculated using the iterative formula for the exact end-to-end heralded non-Gaussian state.

We explore other modes of operation in parameter space by writing down the state heralded across the repeater chain explicitly for $n = 2^x$, $x \in \mathbb{N}$ number of repeater links, denoted as $\hat{\rho}_{A_1 B_n}$, and evaluating its RCI I_R [52]. The rate per channel-use of a M -multiplexed version for the repeater chain R is given by

$$M \times R = I_R(\hat{\rho}_{A_1 B_n}) \times (1 - (1 - p_{\text{sciss}})^M)^{n-1} \times p_{\text{swap}}^{n-1}, \quad (9)$$

where p_{sciss} is the heralding success probability of the quantum scissors in a repeater link and p_{swap} is the entanglement swap success probability associated with the non-Gaussian entangled state projection (inclusive of its physical implementation) for connecting two repeater links. We identified an achievable rate for the scheme by choosing the TMSV mean photon numbers to be 0.0719, the quantum scissors gain according to a power law given by $\kappa = k(\eta^{1/n})^u$, where $k = 0.0557$ and $u = 0.6057$, and the entanglement swap parameter to be $q = 1/\xi$ in relation to (1). Fig. 5 shows the rate curves corresponding to this new mode of operation of the scheme for a degree of multiplexing $M = 10^6$ and different number of repeaters. We find that our scheme now beats C_{direct} already at a

distance of 500 km with just one repeater node. At a distance of 1000 km, the new mode of operation attains the same rate as the DV-like mode of operation for much smaller M (10^6 compared to 10^{13}), confirming that it is significantly better, thereby showcasing the true potential of CV.

Outlook: Some possible directions for future work on CV repeaters include considering the use of other entanglement sources such as the Bell states in the Gottesman-Kitaev-Preskill [53] qubit basis, and other repeater architectures such as the notion of a one-way repeater scheme based on quantum error correction, logical Bell state measurements and teleportation [16]. Also, CV repeaters for more general network scenarios involving multiple communicating parties largely remains to be explored.

Such work might pave the way towards bridging the gap between achievable entanglement distribution rates in repeater networks and the corresponding repeater-assisted end-to-end rate capacities [54] (see also [55]).

This work was supported by the Office of Naval Research program Communications and Networking with Quantum Operationally-Secure Technology for Maritime Deployment (CONQUEST), awarded under Raytheon BBN Technologies prime contract number N00014-16-C-2069, and a subcontract to University of Arizona. This document does not contain technology or technical data controlled under either the U.S. International Traffic in Arms Regulations or the U.S. Export Administration Regulations. KPS thanks Frederic Grosshans and William Munro for helpful discussions.

Supplemental Material for “A continuous variable quantum repeater with quantum scissors”

Kaushik P. Seshadreesan,¹ Hari Krovi,² and Saikat Guha¹

¹*College of Optical Sciences, University of Arizona, Tucson, AZ 85721, USA*

²*Quantum Engineering and Computing Physical Sciences and Systems, Raytheon BBN Technologies, Cambridge, MA 02138, USA*

(Dated: December 15, 2024)

I. A LOWER BOUND ON THE DISTILLABLE ENTANGLEMENT OF THE REPEATER LINK STATE

In this section, we derive the reverse coherent information (RCI) [11, 32–34] of the state heralded across the continuous variable (CV) repeater link in Fig. 1 of the main text for any $N \geq 1$ number of quantum scissors. The RCI is a proven information theoretic lower bound on a state’s distillable entanglement in the asymptotic limit of a large number of copies of the state.

Consider that the two-mode squeezed vacuum (TMSV) state can be expressed in the Fock basis as

$$|\psi\rangle_{AR} = \sqrt{1 - \chi^2} \sum_{n=0}^{\infty} \chi^n |n\rangle_A |n\rangle_R, \quad (S1)$$

where $\chi = \tanh(\sinh^{-1} \sqrt{\mu})$, μ being the mean photon number in each mode. By modeling the pure loss channel of transmissivity t with a beam splitter of the same transmissivity acting on the signal mode R and the environment mode E which is in the vacuum state, we obtain a three-mode output state ($R \rightarrow Y$) of the form

$$|\psi\rangle_{AYE} / \sqrt{1 - \chi^2} = \sum_{n=0}^{\infty} \chi^n \sum_{k=0}^n \sqrt{\binom{n}{k}} x^k y^{n-k} |n\rangle_A |n-k\rangle_Y |k\rangle_E \quad (S2)$$

$$= \sum_{k=0}^{\infty} \sum_{n=k}^{\infty} \chi^n \sqrt{\binom{n}{k}} x^k y^{n-k} |n\rangle_A |n-k\rangle_Y |k\rangle_E \quad (S3)$$

$$= \sum_{k=0}^{\infty} \sum_{m=0}^{\infty} \chi^n \sqrt{\binom{m+k}{k}} x^k y^m |m+k\rangle_A |m\rangle_Y |k\rangle_E, \quad (S4)$$

where $x = \sqrt{1-t}$ and $y = \sqrt{t}$.

When NLA is successfully applied on the mode Y ($Y \rightarrow B$) using N -quantum scissors (c.f. [31, Fig. 1] for a schematic of the NLA), the state heralded across Alice, Bob and the environment, and the heralding success

probability are given by

$$|\psi\rangle_{ABE} = \frac{c}{\sqrt{P_N}} \sum_{k=0}^{\infty} a^k \sum_{m=0}^N \frac{N!}{(N-m)!} \sqrt{\binom{m+k}{k}} b^m \times |m+k\rangle_A |m\rangle_B |k\rangle_E, \quad (\text{S5})$$

$$P_N = c^2 \sum_k a^{2k} \sum_{m=0}^N \left(\frac{N!}{(N-m)!} \right)^2 \binom{m+k}{k} b^{2m}, \quad (\text{S6})$$

where $a = \chi\sqrt{1-t}$, $b = g\chi\sqrt{t}/N$, $c = \sqrt{(1-\chi^2)\kappa^N}$, g is the NLA gain of the quantum scissors, and $\kappa = 1/(1+g^2)$ is an intrinsic parameter in the quantum scissors.

The final two-mode state heralded across the NLA is obtained by tracing over the loss mode E as $\rho_{AB}^{(N)} = \sum_{u=0}^{\infty} \rho_{AB}^{(N)}(u)$, where

$$\rho_{AB}^{(N)}(u) = \sum_{m=0}^N \sum_{m'=0}^N \zeta_{m,u}^{(N)} \zeta_{m',u}^{(N)} |m+u, m\rangle \langle m'+u, m'|_{AB}, \quad (\text{S7})$$

and the coefficients $\zeta_{m,u}$ are given by

$$\zeta_{m,u}^{(N)} = ca^u b^m \frac{N!}{(N-m)!} \sqrt{\binom{m+u}{u}}. \quad (\text{S8})$$

The state $\rho_{AB}^{(N)}$ is thus

$$\rho_{AB}^{(N)} = \sum_{u=0}^{\infty} \sum_{i=0}^N \left(\zeta_{i,u}^{(N)} \right)^2 |\Phi_N(u)\rangle \langle \Phi_N(u)|_{AB} \quad (\text{S9})$$

$$|\Phi_N(u)\rangle_{AB} = \frac{\sum_{i=0}^N \left(\frac{\zeta_{i,u}^{(N)}}{\zeta_{N,u}^{(N)}} \right) |u+i, i\rangle_{AB}}{\sqrt{\sum_{i=0}^N \left(\frac{\zeta_{i,u}^{(N)}}{\zeta_{N,u}^{(N)}} \right)^2}}, \quad (\text{S10})$$

so that its entropy is given by

$$H(AB) = - \sum_{u=0}^{\infty} \left(\sum_{i=0}^N \left(\zeta_{i,u}^{(N)} \right)^2 \right) \log_2 \left(\sum_{i=0}^N \left(\zeta_{i,u}^{(N)} \right)^2 \right). \quad (\text{S11})$$

The state on system A is obtained by tracing over B as $\rho_A^{(N)} = \text{Tr}_B \left(\rho_{AB}^{(N)} \right)$

$$\rho_A^{(N)} = \sum_{u=0}^{\infty} \sum_{m=0}^N \left(\zeta_{m,u}^{(N)} \right)^2 |m+u\rangle \langle m+u|_A \quad (\text{S12})$$

$$= \left(\sum_{u=0}^N \Gamma_1(u) + \sum_{u=N+1}^{\infty} \Gamma_2(u) \right) |u\rangle \langle u|_A. \quad (\text{S13})$$

where

$$\Gamma_1(u) = \sum_{\substack{\{i,j\} \geq 0, \\ i+j=u}} \left(\zeta_{i,j}^{(N)} \right)^2, \quad \Gamma_2(u) = \sum_{i=0}^N \left(\zeta_{i,u-i}^{(N)} \right)^2. \quad (\text{S14})$$

Its entropy is therefore given by

$$H(A) = - \sum_{u=0}^N \Gamma_1(u) \log_2 \Gamma_1(u) - \sum_{u=N+1}^{\infty} \Gamma_2(u) \log_2 \Gamma_2(u). \quad (\text{S15})$$

Thus, the RCI of the heralded state follows from (S11) and (S15) as

$$I_R = H(A) - H(AB). \quad (\text{S16})$$

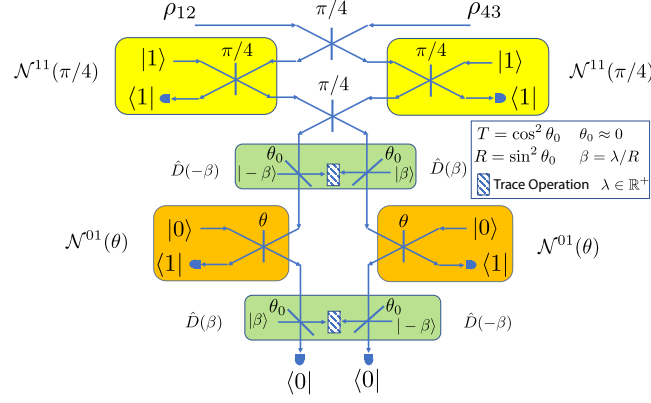


Figure S1. A Non-Gaussian entanglement swap operation based on Fock state filtering, displacement operations, photon subtraction and vacuum projection.

II. NON-GAUSSIAN ENTANGLEMENT SWAP

A beam splitter of transmissivity $T = \cos^2 \theta$ acting on modes i and j can be described by the unitary operator:

$$U_{ij}(\theta) = \exp\left(-\theta\left(\hat{a}_i^\dagger \hat{a}_j - \hat{a}_j^\dagger \hat{a}_i\right)\right), \quad (\text{S17})$$

that transforms the mode operators as

$$\begin{pmatrix} \hat{a}_i \\ \hat{a}_j \end{pmatrix} \rightarrow U_{ij}(\theta)^\dagger \begin{pmatrix} \hat{a}_i \\ \hat{a}_j \end{pmatrix} U_{ij}(\theta) \quad (\text{S18})$$

$$= \begin{pmatrix} \cos \theta & \sin \theta \\ -\sin \theta & \cos \theta \end{pmatrix} \begin{pmatrix} \hat{a}_i \\ \hat{a}_j \end{pmatrix}. \quad (\text{S19})$$

It's action on a Fock state input $|n\rangle_i \otimes |0\rangle_j$ is given by

$$U_{ij}(\theta) |n\rangle_i |0\rangle_j = \sum_{k=0}^n \sqrt{\binom{n}{k}} (\cos^2 \theta)^{k/2} (\sin^2 \theta)^{(n-k)/2} |k\rangle_i |n-k\rangle_j. \quad (\text{S20})$$

Proposition 1. Consider the channel comprising of mixing an input mode i with a mode j in the Fock state $|1\rangle_j$ on a beam splitter $U_{ij}(\theta)$, followed by a projective measurement $\langle 1|_i$ in mode i . Let us denote this non-trace-preserving map as $\mathcal{N}_{i \rightarrow j}^{11}(\theta)$. It can be written as

$$\mathcal{N}_{i \rightarrow j}^{11}(\theta) = \left(-\sin \theta + \cos \theta \frac{d}{d\theta}\right) (\sin \theta)^{\hat{n}_{ij}}, \quad (\text{S21})$$

where we use the notation $\hat{n}_{ij} |n\rangle_i = |n\rangle_j$ to denote input to output transformation.

Proof. We have

$$U_{ij}(\theta) |n\rangle_i |1\rangle_j = U_{ij}(\theta) \hat{a}_j^\dagger |n\rangle_i |0\rangle_j \quad (\text{S22})$$

$$= \left(-\sin \theta \hat{a}_i^\dagger + \cos \theta \hat{a}_j^\dagger\right) U_{ij}(\theta) |n\rangle_i |0\rangle_j \quad (\text{S23})$$

This implies

$$\langle 1|_i U_{ij}(\theta) |n\rangle_i |1\rangle_j = \langle 0|_i \hat{a}_i \left(-\sin \theta \hat{a}_i^\dagger + \cos \theta \hat{a}_j^\dagger \right) U_{ij}(\theta) |n\rangle_i |0\rangle_j \quad (\text{S24})$$

$$= -\sin \theta \langle 0|_i \hat{a}_i \hat{a}_i^\dagger U_{ij}(\theta) |n\rangle_i |0\rangle_j + \cos \theta \langle 0|_i \hat{a}_i \hat{a}_j^\dagger U_{ij}(\theta) |n\rangle_i |0\rangle_j \quad (\text{S25})$$

$$= -\sin \theta \langle 0|_i \left(1 + \hat{a}_i^\dagger \hat{a}_i \right) U_{ij}(\theta) |n\rangle_i |0\rangle_j + \cos \theta \langle 0|_i \hat{a}_i \hat{a}_j^\dagger U_{ij}(\theta) |n\rangle_i |0\rangle_j \quad (\text{S26})$$

$$= -\sin \theta \langle 0|_i U_{ij}(\theta) |n\rangle_i |0\rangle_j + \cos \theta \langle 0|_i \hat{a}_i \hat{a}_j^\dagger U_{ij}(\theta) |n\rangle_i |0\rangle_j \quad (\text{S27})$$

$$= -\sin^{n+1} \theta |n\rangle_j + n \cos^2 \theta \sin^{n-1} \theta |n\rangle_j \quad (\text{S28})$$

$$= \left(-\sin \theta + \cos \theta \frac{d}{d\theta} \right) \sin^n \theta |n\rangle_j, \quad (\text{S29})$$

which implies, for a general state $|\psi\rangle_i = \sum_n c_n |n\rangle_i$, the action of the channel is as given in (S21). \square

Proposition 2. Consider the channel comprising of mixing an input mode i with a mode j in the Fock state $|0\rangle_j$ on a beam splitter $U_{ij}(\theta)$, followed by a projective measurement $\langle 1|_i$ in the mode i . Let us denote this non-trace-preserving map as $\mathcal{N}_{i \rightarrow j}^{01}(\theta)$. It can be written as

$$\mathcal{N}_{i \rightarrow j}^{01}(\theta) = \cos \theta (\sin \theta)^{\hat{n}_{ij}} \hat{a}_j \quad (\text{S30})$$

where we use the notation $\hat{n}_{ij} |n\rangle_i = |n\rangle_j$ to denote the input to output transformation.

Proof. From (S20), we have

$$\langle 1|_i U_{ij}(\theta) |n\rangle_i |0\rangle_j = \sqrt{n} \cos \theta \sin^{n-1} \theta |n-1\rangle_j \quad (\text{S31})$$

$$= \hat{a}_j \cos \theta \sin^{n-1} \theta |n\rangle_j \quad (\text{S32})$$

$$= \cos \theta (\sin \theta)^{\hat{n}_{ij}} \hat{a}_j |n\rangle_j \quad (\text{S33})$$

which implies, for a general state $|\psi\rangle_i = \sum_n c_n |n\rangle_i$, the action of the channel is as given in (S30). \square

Remark 3. The displacement operation $\hat{D}_i(\lambda)$ on a mode i can be implemented using a beam splitter $U_{ij}(\theta)$ with the mode j in the coherent state $|\lambda/\sin^2 \theta\rangle_j$.

Proposition 4. Consider the measurement depicted in Fig. S1. The projection implemented by the measurement scheme on modes 2 and 3 is given by \hat{F}_{23}^\dagger , where

$$\hat{F}_{23} = -\cos^2 \theta (\sin^2 \theta)^{\lambda^2} \left(\frac{\lambda^2}{2} |0\rangle_2 |0\rangle_3 + \frac{1}{4} |1\rangle_2 |1\rangle_3 \right), \quad (\text{S34})$$

where θ is related to the transmissivity of the photon subtraction beam splitters and λ is the amplitude of the displacement stages.

Proof. The measurement scheme depicted in Fig. 1 implements the projection \hat{F}_{23}^\dagger , which is

$$\langle 0, 0|_{23} \hat{D}_3(-\lambda) \mathcal{N}_{3 \rightarrow 3'}^{01}(\theta)_{\theta \rightarrow 0} \hat{D}_3(\lambda) \hat{D}_2(\lambda) \mathcal{N}_{2 \rightarrow 2'}^{01}(\theta)_{\theta \rightarrow 0} \hat{D}_2(-\lambda) U_{23}^\dagger(\pi/4) \mathcal{N}_{2 \rightarrow 2'}^{11}(\pi/4) \mathcal{N}_{3 \rightarrow 3'}^{11}(\pi/4) U_{23}(\pi/4), \quad (\text{S35})$$

where for brevity of notation the primes on the output modes of individual elements in the transformation are suppressed ahead of the subsequent elements, and $\lambda \in \mathbf{R}^+$.

From, (S30), we have

$$\langle 0|_2 \hat{D}_2(\lambda) (\mathcal{N}_{2 \rightarrow 2'}^{01}(\theta)) \hat{D}_2(-\lambda) = \langle 0|_2 \hat{D}_2(\lambda) \cos \theta (\sin \theta)^{\hat{n}_2} \hat{a}_2 \hat{D}_2(-\lambda) \quad (\text{S36})$$

$$= \cos \theta (\sin \theta)^{\lambda^2} \langle -\lambda|_2 \hat{a}_2 \hat{D}_2(-\lambda) \quad (\text{S37})$$

$$= \cos \theta (\sin \theta)^{\lambda^2} \langle 0|_2 \hat{D}_2(\lambda) \hat{a}_2 \hat{D}_2(-\lambda) \quad (\text{S38})$$

$$= \cos \theta (\sin \theta)^{\lambda^2} \langle 0|_2 (\hat{a}_2 - \lambda) \quad (\text{S39})$$

$$= \cos \theta (\sin \theta)^{\lambda^2} (\langle 1|_2 - \lambda \langle 0|_2). \quad (\text{S40})$$

Likewise,

$$\langle 0|_3 \hat{D}_3(-\lambda) (\mathcal{N}_{3 \rightarrow 3''}^{01}(\theta)) \hat{D}_3(\lambda) = \cos \theta (\sin \theta)^{\lambda^2} (\langle 1|_3 + \lambda \langle 0|_3).$$

From (S21),

$$\mathcal{N}^{11}(\pi/4) |n\rangle = -\left(\frac{1}{\sqrt{2}}\right)^{n+1} + n \left(\frac{1}{\sqrt{2}}\right)^2 \left(\frac{1}{\sqrt{2}}\right)^{n-1} |n\rangle \quad (\text{S41})$$

$$= \frac{(n-1)}{(\sqrt{2})^{n+1}} |n\rangle. \quad (\text{S42})$$

Therefore, we have

$$\mathcal{N}^{11}(\pi/4) = \frac{(\hat{n}-1)}{(\sqrt{2})^{\hat{n}+1}}.$$

Thus, \hat{F}_{23}^\dagger in (S35) can be written as

$$\hat{F}_{23}^\dagger = \cos^2 \theta (\sin^2 \theta)^{\lambda^2} (\langle 1|_3 + \lambda \langle 0|_3) (\langle 1|_2 - \lambda \langle 0|_2) U_{23}^\dagger(\pi/4) \frac{(\hat{n}_2-1)}{(\sqrt{2})^{\hat{n}_2+1}} \frac{(\hat{n}_3-1)}{(\sqrt{2})^{\hat{n}_3+1}} U_{23}(\pi/4) \quad (\text{S43})$$

$$= \cos^2 \theta (\sin^2 \theta)^{\lambda^2} (\langle 1|_3 + \lambda \langle 0|_3) (\langle 1|_2 - \lambda \langle 0|_2) U_{23}^\dagger(\pi/4) (\hat{n}_2-1) \frac{1}{(\sqrt{2})^{\hat{n}_2+\hat{n}_3+2}} (\hat{n}_3-1) U_{23}(\pi/4) \quad (\text{S44})$$

$$= \cos^2 \theta (\sin^2 \theta)^{\lambda^2} (\langle 1|_3 + \lambda \langle 0|_3) (\langle 1|_2 - \lambda \langle 0|_2) \times U_{23}^\dagger(\pi/4) (\hat{n}_2-1) U_{23}(\pi/4) U_{23}^\dagger(\pi/4) \frac{1}{(\sqrt{2})^{\hat{n}_2+\hat{n}_3+2}} U_{23}(\pi/4) U_{23}^\dagger(\pi/4) (\hat{n}_3-1) U_{23}(\pi/4). \quad (\text{S45})$$

From (S19), we have

$$U_{23}^\dagger(\pi/4) (\hat{n}_3-1) U_{23}(\pi/4) = \frac{(\hat{a}_2^\dagger - \hat{a}_3^\dagger)(\hat{a}_2 - \hat{a}_3)}{2} - 1 \quad (\text{S46})$$

$$U_{23}^\dagger(\pi/4) (\hat{n}_2-1) U_{23}(\pi/4) = \frac{(\hat{a}_2^\dagger + \hat{a}_3^\dagger)(\hat{a}_2 + \hat{a}_3)}{2} - 1. \quad (\text{S47})$$

Thus, we have \hat{F}_{23}^\dagger

$$= \cos^2 \theta (\sin^2 \theta)^{\lambda^2} (\langle 1|_3 + \lambda \langle 0|_3) (\langle 1|_2 - \lambda \langle 0|_2) \left(\frac{(\hat{a}_2^\dagger + \hat{a}_3^\dagger)(\hat{a}_2 + \hat{a}_3)}{2} - 1 \right) \frac{1}{(\sqrt{2})^{\hat{n}_3+\hat{n}_2+2}} \left(\frac{(\hat{a}_2^\dagger - \hat{a}_3^\dagger)(\hat{a}_2 - \hat{a}_3)}{2} - 1 \right).$$

The projector can be written in the ket form as \hat{F}_{23}

$$\begin{aligned} &= \cos^2 \theta (\sin^2 \theta)^{\lambda^2} \left(\frac{(\hat{a}_2^\dagger + \hat{a}_3^\dagger)(\hat{a}_2 + \hat{a}_3)}{2} - 1 \right) \frac{1}{(\sqrt{2})^{\hat{n}_3+\hat{n}_2+2}} \left(\frac{(\hat{a}_2^\dagger - \hat{a}_3^\dagger)(\hat{a}_2 - \hat{a}_3)}{2} - 1 \right) (|1\rangle_2 - \lambda |0\rangle_2) (|1\rangle_3 + \lambda |0\rangle_3) \\ &= \cos^2 \theta (\sin^2 \theta)^{\lambda^2} \left(\frac{(\hat{a}_2^\dagger + \hat{a}_3^\dagger)(\hat{a}_2 + \hat{a}_3) - 2}{8} \right) \left(-\frac{1}{\sqrt{2}} (|2\rangle_2 |0\rangle_3 + |0\rangle_2 |2\rangle_3) + 2\lambda^2 |0\rangle_2 |0\rangle_3 \right) \\ &= -\cos^2 \theta (\sin^2 \theta)^{\lambda^2} \left(\frac{\lambda^2}{2} |0\rangle_2 |0\rangle_3 + \frac{1}{4} |1\rangle_2 |1\rangle_3 \right). \end{aligned} \quad (\text{S48})$$

□

Remark 5. \hat{F}_{23} can be expressed in a weighted normalized form as

$$\left(\frac{-\cos^2 \theta (\sin^2 \theta)^{\lambda^2} \sqrt{1+4\lambda^4}}{4} \right) \left(\frac{2\lambda^2 |0\rangle_2 |0\rangle_3 + |1\rangle |1\rangle_3}{\sqrt{1+4\lambda^4}} \right).$$

Remark 6. Thus, states

$$|\psi\rangle_{12} = \frac{|0\rangle_1 |0\rangle_2 + \xi |1\rangle_1 |1\rangle_2}{\sqrt{1+\xi^2}},$$

$$|\psi\rangle_{43} = \frac{|0\rangle_4 |0\rangle_3 + \xi |1\rangle_4 |1\rangle_3}{\sqrt{1+\xi^2}},$$

can be entanglement swapped into a state $|\psi\rangle_{14} = (|0\rangle_1 |0\rangle_4 + \xi |1\rangle_1 |1\rangle_4) / \sqrt{1+\xi^2}$, using \hat{F}_{23} of Prop. 4 with $\lambda = \sqrt{\xi/2}$. The success probability of physically implementing the projection \hat{F}_{23} on these states is given by

$$P_{phys} = \left(\frac{\xi^2}{1+\xi^2} \right) \frac{\cos^4 \theta (\sin^2 \theta)^\xi}{16}, \quad (\text{S49})$$

which can be numerically optimized over the reflectivity parameter θ .

III. ITERATIVE FORMULA FOR A CHAIN OF REPEATER LINKS CONNECTED BY THE NON-GAUSSIAN ENTANGLEMENT SWAP

As an alternative to the Fock basis description presented in Section 1, the state successfully heralded across the proposed CV repeater link with a single quantum scissors can also be expressed as [48]

$$|\psi^{(1)}\rangle_{A_1 B_1 L_1} = \frac{1}{\gamma^{(1)}} \left(\gamma_0^{(1)} + \gamma_1^{(1)} a_1^\dagger + \gamma_2^{(1)} b_1^\dagger + \gamma_3^{(1)} a_1^\dagger b_1^\dagger \right) \sigma_{A_1 L_1}^\rho |0\rangle_{A_1 B_1 L_1}, \quad (\text{S50})$$

where

$$\gamma_0^{(1)} = f, \quad (\text{S51})$$

$$\gamma_1^{(1)} = 0, \quad (\text{S52})$$

$$\gamma_2^{(1)} = 0, \quad (\text{S53})$$

$$\gamma_3^{(1)} = \kappa_h f \quad (\text{S54})$$

$$f = \frac{\sqrt{\kappa} \operatorname{sech} r}{\sqrt{\operatorname{sech}^2 r + t \tanh^2 r}}, \quad (\text{S55})$$

$$\gamma^{(1)} = \sqrt{\frac{\kappa \operatorname{sech}^2 r + t \tanh^2 r}{\cosh^2 r (\operatorname{sech}^2 r + t \tanh^2 r)^2}}, \quad (\text{S56})$$

$$\kappa_h = \sqrt{\frac{1-\kappa}{\kappa}} \sqrt{t} \tanh r, \quad (\text{S57})$$

$$\tanh \rho = \sqrt{1-t} \tanh r, \quad (\text{S58})$$

σ_{AL}^ρ is the two-mode squeezing operator corresponding to squeezing of magnitude ρ in modes A_1 , L_1 , and $r = (\sinh^{-1} \sqrt{\mu})$. The heralding probability is given by

$$P_{sciss} = \gamma^{(1)2}. \quad (\text{S59})$$

The state obtained by connecting two such repeater links using a Bell swap projection $\hat{\Pi}_{B_1 A_2} = |\phi\rangle\langle\phi|_{B_1 A_2}$, where

$$|\phi\rangle_{B_1 A_2} = \frac{1}{\sqrt{1+q^2}} (|00\rangle_{B_1 A_2} + q|11\rangle_{B_1 A_2}), \quad q \in \mathbb{R}^+, \quad (\text{S60})$$

is given by

$$\langle \phi |_{B_1 A_2} | \psi^{(1)} \rangle_{A_1 B_1 L_1} \otimes | \psi^{(1)} \rangle_{A_2 B_2 L_2} = \langle \phi |_{B_1 A_2} \left(\left(\frac{f}{\gamma^{(1)}} \right)^2 (1 + \kappa a_1^\dagger b_1^\dagger)(1 + \kappa a_2^\dagger b_2^\dagger) \sigma_{A_1 L_1}^\rho \sigma_{A_2 L_2}^\rho | 0 \rangle_{A_1 B_1 L_1 A_2 B_2 L_2} \right). \quad (\text{S61})$$

As a result, the state of the modes A_1 , B_2 , L_1 is heralded as

$$| \psi^{(2)} \rangle_{A_1 B_2 L_1} = \frac{1}{\gamma^{(2)}} \left(\gamma_0^{(2)} + \gamma_1^{(2)} a_1^\dagger + \gamma_2^{(2)} b_2^\dagger + \gamma_3^{(2)} a_1^\dagger b_2^\dagger \right) \sigma_{A_1 L_1}^\rho | 0 \rangle_{A_1 B_2 L_1}, \quad (\text{S62})$$

where

$$\gamma_0^{(2)} = 1, \quad (\text{S63})$$

$$\gamma_1^{(2)} = \kappa_h q \tanh \rho \quad (\text{S64})$$

$$\gamma_2^{(2)} = 0 \quad (\text{S65})$$

$$\gamma_3^{(2)} = \kappa_h^2 q \quad (\text{S66})$$

$$\gamma^{(2)} = \sqrt{1 + \kappa_h^2 q^2 \sinh^2 \rho + \kappa_h^4 q^2 \cosh^2 \rho}. \quad (\text{S67})$$

The corresponding success probability is given by the product of the ideal Bell swap projection probability for the repeater link states $P_{\hat{\Pi}}$ times the probability of physically implementing the projection using linear optics P_{phys} of (S49), i.e.,

$$P_{\text{swap}} = P_{\hat{\Pi}} \times P_{\text{phys}}, \quad (\text{S68})$$

where the former is the norm of the unnormalized state in (S61), given by

$$P_{\hat{\Pi}} = \frac{f^4 \text{sech}^2 \rho}{(1 + q^2) \gamma^{(1)4}} \gamma^{(2)2} \quad (\text{S69})$$

Now, say we want to concatenate two such states $| \psi^{(2)} \rangle_{ABL}$ (connected by the non-Gaussian Bell state projection), to obtain the state $| \psi^{(3)} \rangle_{ABL}$ across four repeater links, or similarly concatenate two states $| \psi^{(3)} \rangle_{ABL}$ to obtain the state across eight repeater links $| \psi^{(4)} \rangle_{ABL}$. More generally, assume that at the i^{th} step of concatenation, we have two states whose tensor product is

$$| \psi^{(i)} \rangle_{A_1 B_1 L_1} \otimes | \psi^{(i)} \rangle_{A_2 B_2 L_2} = (\gamma_0^{(i)} + \gamma_1^{(i)} a_1^\dagger + \gamma_2^{(i)} b_1^\dagger + \gamma_3^{(i)} a_1^\dagger b_1^\dagger) (\gamma_0^{(i)} + \gamma_1^{(i)} a_2^\dagger + \gamma_2^{(i)} b_2^\dagger + \gamma_3^{(i)} a_2^\dagger b_2^\dagger) \sigma_{A_1 L_1}^\rho \sigma_{A_2 L_2}^\rho | 0 \rangle_{A_1 B_1 L_1 A_2 B_2 L_2}, \quad (\text{S70})$$

where for brevity of notation, we have denoted the modes as A_1 , B_1 , L_1 , A_2 , B_2 , L_2 in place of the actual mode labels. When the modes B_1 and A_2 are projected on the non-Gaussian Bell state, we have

$$\langle \phi |_{B_1 A_2} | \psi^{(i)} \rangle_{A_1 B_1 L_1} \otimes | \psi^{(i)} \rangle_{A_2 B_2 L_2} = (a \langle 00 |_{B_1 A_2} + b \langle 01 |_{B_1 A_2} + c \langle 10 |_{B_1 A_2} + d \langle 11 |_{B_1 A_2}) \sigma_{A_1 L_1}^\rho \sigma_{A_2 L_2}^\rho | 0 \rangle_{A_1 B_1 L_1 A_2 B_2 L_2}, \quad (\text{S71})$$

where

$$a = \frac{(\gamma_0^{(i)} + \gamma_1^{(i)} a_1^\dagger)(\gamma_0^{(i)} + \gamma_2^{(i)} b_2^\dagger)}{\sqrt{1 + q^2}} + \frac{(\gamma_2^{(i)} + \gamma_3^{(i)} a_1^\dagger)(\gamma_1^{(i)} + \gamma_3^{(i)} b_2^\dagger)q}{\sqrt{1 + q^2}} \quad (\text{S72})$$

$$b = \frac{(\gamma_2^{(i)} + \gamma_3^{(i)} a_1^\dagger)(\gamma_0^{(i)} + \gamma_2^{(i)} b_2^\dagger)q}{\sqrt{1 + q^2}} \quad (\text{S73})$$

$$c = \frac{(\gamma_0^{(i)} + \gamma_1^{(i)} a_1^\dagger)(\gamma_1^{(i)} + \gamma_3^{(i)} b_2^\dagger)q}{\sqrt{1 + q^2}} \quad (\text{S74})$$

$$d = \frac{(\gamma_0^{(i)} + \gamma_1^{(i)} a_1^\dagger)(\gamma_0^{(i)} + \gamma_2^{(i)} b_2^\dagger)q}{\sqrt{1 + q^2}}. \quad (\text{S75})$$

The resulting state that is heralded in modes A_1 , B_2 , L_1 is given by

$$|\psi^{(i+1)}\rangle_{A_1 B_2 L_1} = \frac{1}{\gamma^{(i+1)}} \left(\gamma_0^{(i+1)} + \gamma_1^{(i+1)} a_1^\dagger + \gamma_2^{(i+1)} b_2^\dagger + \gamma_2^{(i+1)} a_1^\dagger b_2^\dagger \right) \sigma_{A_1 L_1}^\rho |0\rangle, \quad (\text{S76})$$

where

$$\gamma_0^{(i+1)} = \left(\gamma_0^{(i)^2} + q \gamma_2^{(i)} (\gamma_1^{(i)} + \gamma_0^{(i)} \tanh p) \right) \quad (\text{S77})$$

$$\gamma_1^{(i+1)} = \left(\gamma_0^{(i)} \gamma_1^{(i)} + q \gamma_3^{(i)} (\gamma_1^{(i)} + \gamma_0^{(i)} \tanh \rho) \right) \quad (\text{S78})$$

$$\gamma_2^{(i+1)} = \left(\gamma_0^{(i)} \gamma_2^{(i)} + q \gamma_2^{(i)} (\gamma_3^{(i)} + \gamma_2^{(i)} \tanh \rho) \right) \quad (\text{S79})$$

$$\gamma_3^{(i+1)} = \left(\gamma_1^{(i)} \gamma_2^{(i)} + q \gamma_3^{(i)} (\gamma_3^{(i)} + \gamma_2^{(i)} \tanh \rho) \right), \quad (\text{S80})$$

$$\gamma^{(i+1)} = \sqrt{\left(\gamma_0^{(i+1)^2} + \gamma_2^{(i+1)^2} \right) + \cosh^2 \rho \left(\gamma_1^{(i+1)^2} + \gamma_3^{(i+1)^2} \right)}. \quad (\text{S81})$$

The state can be simplified as

$$|\psi^{(i+1)}\rangle_{A_1 B_2 L_1} = \frac{1}{\gamma^{(i+1)}} \left[\left(\gamma_0^{(i+1)} + \gamma_1^{(i+1)} a_1^\dagger \right) \sigma_{A_1 L_1}^\rho |0\rangle_{A_1 L_1} \otimes |0\rangle_{B_2} + \left(\gamma_2^{(i+1)} + \gamma_3^{(i+1)} a_1^\dagger \right) \sigma_{A_1 L_1}^\rho |0\rangle_{A_1 L_1} \otimes |1\rangle_{B_2} \right] \quad (\text{S82})$$

The end-to-end two-mode state heralded across a repeater chain of $n = 2^x$, $x \in \mathbb{N}$, repeater links can be written down by tracing over the environment mode as

$$\begin{aligned} \hat{\rho}_{A_1 B_{2^x}} &= \text{Tr}_{L_1} \left(|\psi^{(x+1)}\rangle \langle \psi^{(x+1)}|_{A_1 B_{2^x} L_1} \right) \\ &= \hat{\rho}_{A_1}^{(0,0)} \otimes |0\rangle \langle 0|_{B_{2^x}} + \hat{\rho}_{A_1}^{(0,1)} \otimes |0\rangle \langle 1|_{B_{2^x}} + \hat{\rho}_{A_1}^{(1,0)} \otimes |1\rangle \langle 0|_{B_{2^x}} + \hat{\rho}_{A_1}^{(1,1)} \otimes |1\rangle \langle 1|_{B_{2^x}}, \end{aligned} \quad (\text{S83})$$

where

$$\begin{aligned} \hat{\rho}_{A_1}^{(0,0)} &= \frac{1}{\gamma^{(x+1)^2}} \left(\gamma_0^{(x+1)} + \gamma_1^{(x+1)} a_1^\dagger \right) \hat{\rho}_{A_1}^{th}(\rho) \left(\gamma_0^{(x+1)} + \gamma_1^{(x+1)} a_1 \right) \\ \hat{\rho}_{A_1}^{(0,1)} &= \frac{1}{\gamma^{(x+1)^2}} \left(\gamma_0^{(x+1)} + \gamma_1^{(x+1)} a_1^\dagger \right) \hat{\rho}_{A_1}^{th}(\rho) \left(\gamma_2^{(x+1)} + \gamma_3^{(x+1)} a_1 \right) \\ \hat{\rho}_{A_1}^{(1,0)} &= \frac{1}{\gamma^{(x+1)^2}} \left(\gamma_2^{(x+1)} + \gamma_3^{(x+1)} a_1^\dagger \right) \hat{\rho}_{A_1}^{th}(\rho) \left(\gamma_0^{(x+1)} + \gamma_1^{(x+1)} a_1 \right) \\ \hat{\rho}_{A_1}^{(1,1)} &= \frac{1}{\gamma^{(x+1)^2}} \left(\gamma_2^{(x+1)} + \gamma_3^{(x+1)} a_1^\dagger \right) \hat{\rho}_{A_1}^{th}(\rho) \left(\gamma_2^{(x+1)} + \gamma_3^{(x+1)} a_1 \right), \end{aligned} \quad (\text{S84})$$

where $\hat{\rho}^{th}$ is the thermal state of mean photon number ρ . The above density operator can be written in the Fock basis with terms $\langle m_1, m_2 |_{A_1 B_{2^x}} \cdot \hat{\rho}_{A_1 B_{2^x}} \cdot | n_1, n_2 \rangle_{A_1 B_{2^x}} = \hat{\rho}_{A_1}^{(m_2, n_2)}$, $\{m_1, n_1 \in \mathbb{W}\}$ and $\{m_2, n_2 \in \{0, 1\}\}$, where

$$\begin{aligned} \hat{\rho}_{A_1}^{(0,0)} &= \langle \phi_{m_1}^{(0)} | \hat{\rho}_{A_1}^{th}(\rho) | \phi_{n_1}^{(0)} \rangle \\ \hat{\rho}_{A_1}^{(0,1)} &= \langle \phi_{m_1}^{(0)} | \hat{\rho}_{A_1}^{th}(\rho) | \phi_{n_1}^{(1)} \rangle \\ \hat{\rho}_{A_1}^{(1,0)} &= \langle \phi_{m_1}^{(1)} | \hat{\rho}_{A_1}^{th}(\rho) | \phi_{n_1}^{(0)} \rangle \\ \hat{\rho}_{A_1}^{(1,1)} &= \langle \phi_{m_1}^{(1)} | \hat{\rho}_{A_1}^{th}(\rho) | \phi_{n_1}^{(1)} \rangle, \end{aligned} \quad (\text{S85})$$

with

$$\begin{aligned} |\phi_n^{(0)}\rangle &= \left(\gamma_0^{(x+1)} |n\rangle + \gamma_1^{(x+1)} \sqrt{n} |n-1\rangle \right) / \gamma^{(x+1)}, \\ |\phi_n^{(1)}\rangle &= \left(\gamma_2^{(x+1)} |n\rangle + \gamma_3^{(x+1)} \sqrt{n} |n-1\rangle \right) / \gamma^{(x+1)}. \end{aligned} \quad (\text{S86})$$

Finally, the RCI of the state can thus be calculated from the eigenspectra of the suitably truncated Fock basis density matrices corresponding to $\hat{\rho}_{A_1 B_2 x}$ and $\hat{\rho}_{A_1}$.

-
- [1] H. J. Kimble, *Nature* **453**, 1023 (2008).
 - [2] N. Gisin and R. Thew, *Nature Photonics* **1**, 165 (2007).
 - [3] V. Scarani, H. Bechmann-Pasquinucci, N. J. Cerf, M. Dušek, N. Lütkenhaus, and M. Peev, *Rev. Mod. Phys.* **81**, 1301 (2009).
 - [4] T. J. Proctor, P. A. Knott, and J. A. Dunningham, *Phys. Rev. Lett.* **120**, 080501 (2018).
 - [5] W. Ge, K. Jacobs, Z. Eldredge, A. V. Gorshkov, and M. Foss-Feig, *Phys. Rev. Lett.* **121**, 043604 (2018).
 - [6] Q. Zhuang, Z. Zhang, and J. H. Shapiro, *Phys. Rev. A* **97**, 032329 (2018).
 - [7] R. V. Meter and S. J. Devitt, *Computer* **49**, 31 (2016).
 - [8] V. Danos, E. D'Hondt, E. Kashefi, and P. Panangaden, *Electronic Notes in Theoretical Computer Science* **170**, 73 (2007), proceedings of the 3rd International Workshop on Quantum Programming Languages (QPL 2005).
 - [9] H. Buhrman and H. Röhrig, in *Mathematical Foundations of Computer Science 2003*, edited by B. Rovan and P. Vojtáš (Springer Berlin Heidelberg, Berlin, Heidelberg, 2003) pp. 1–20.
 - [10] M. Takeoka, S. Guha, and M. M. Wilde, *Nature Communications* **5**, 1 (2014), arXiv:1504.06390.
 - [11] S. Pirandola, R. García-Patrón, S. L. Braunstein, and S. Lloyd, *Phys. Rev. Lett.* **102**, 050503 (2009).
 - [12] S. Pirandola, R. Laurenza, C. Ottaviani, and L. Banchi, *Nature Communications* **8**, 15043 (2017).
 - [13] M. M. Wilde, M. Tomamichel, and M. Berta, *IEEE Transactions on Information Theory* **63**, 1792 (2017).
 - [14] W. J. Munro, K. Azuma, K. Tamaki, and K. Nemoto, *IEEE Journal of Selected Topics in Quantum Electronics* **21** (2015), 10.1109/JSTQE.2015.2392076.
 - [15] H.-J. Briegel, W. Dür, J. I. Cirac, and P. Zoller, *Phys. Rev. Lett.* **81**, 5932 (1998).
 - [16] S. Muralidharan, L. Li, J. Kim, N. Lütkenhaus, M. D. Lukin, and L. Jiang, *Scientific Reports* **6**, 20463 (2016).
 - [17] S. Guha, H. Krovi, C. A. Fuchs, Z. Dutton, J. A. Slater, C. Simon, and W. Tittel, *Phys. Rev. A* **92**, 022357 (2015).
 - [18] N. Sinclair, E. Saglamyurek, H. Mallahzadeh, J. A. Slater, M. George, R. Ricken, M. P. Hedges, D. Oblak, C. Simon, W. Sohler, and W. Tittel, *Phys. Rev. Lett.* **113**, 053603 (2014).
 - [19] M. Pant, H. Krovi, D. Englund, and S. Guha, *Phys. Rev. A* **95**, 012304 (2017).
 - [20] K. Azuma, K. Tamaki, and H.-K. Lo, *Nature Communications* **6**, 6787 (2015).
 - [21] R. Namiki, O. Gittsovich, S. Guha, and N. Lütkenhaus, *Phys. Rev. A* **90**, 062316 (2014).
 - [22] J. Hoelscher-Obermaier and P. van Loock, *Phys. Rev. A* **83**, 012319 (2011).
 - [23] T. C. Ralph and A. P. Lund, *AIP Conference Proceedings* **1110**, 155 (2009), <https://aip.scitation.org/doi/pdf/10.1063/1.3131295>.
 - [24] T. C. Ralph, *Phys. Rev. A* **84**, 022339 (2011).
 - [25] D. T. Pegg, L. S. Phillips, and S. M. Barnett, *Phys. Rev. Lett.* **81**, 1604 (1998).
 - [26] J. Dias and T. C. Ralph, *Phys. Rev. A* **95**, 022312 (2017).
 - [27] J. Dias and T. C. Ralph, *Phys. Rev. A* **97**, 032335 (2018).
 - [28] G. Vidal and R. F. Werner, *Phys. Rev. A* **65**, 032314 (2002).
 - [29] M. B. Plenio, *Phys. Rev. Lett.* **95**, 090503 (2005).
 - [30] C. H. Bennett, D. P. DiVincenzo, J. A. Smolin, and W. K. Wootters, *Phys. Rev. A* **54**, 3824 (1996).
 - [31] K. P. Seshadreesan, H. Krovi, and S. Guha, *Phys. Rev. A* **100**, 022315 (2019).
 - [32] R. García-Patrón, S. Pirandola, S. Lloyd, and J. H. Shapiro, *Phys. Rev. Lett.* **102**, 210501 (2009).
 - [33] I. Devetak, M. Junge, C. King, and M. B. Ruskai, *Communications in Mathematical Physics* **266**, 37 (2006).
 - [34] I. Devetak and A. Winter, *Proceedings of the Royal Society of London A: Mathematical, Physical and Engineering Sciences* **461**, 207 (2005).
 - [35] M. Horodecki, P. Horodecki, and R. Horodecki, *Phys. Rev. Lett.* **85**, 433 (2000).
 - [36] S. Tserkis, J. Dias, and T. C. Ralph, “Simulation of Gaussian channels via teleportation and error correction of Gaussian states,” (2018), arXiv:1803.03516v2, 1803.03516.
 - [37] R. Blandino, A. Leverrier, M. Barbieri, J. Etessé, P. Grangier, and R. Tualle-Broui, *Phys. Rev. A* **86**, 012327 (2012).
 - [38] M. Ghalaii, C. Ottaviani, R. Kumar, S. Pirandola, and M. Razavi, “Long-distance continuous-variable quantum key distribution with quantum scissors,” (2018), arXiv:1808.01617v1, 1808.01617.
 - [39] F. Furrer and W. J. Munro, *Phys. Rev. A* **98**, 032335 (2018).
 - [40] J. Fiurášek, *Phys. Rev. A* **82**, 042331 (2010).
 - [41] D. E. Browne, J. Eisert, S. Scheel, and M. B. Plenio, *Phys. Rev. A* **67**, 062320 (2003).
 - [42] S. K. Özdemir, A. Miranowicz, M. Koashi, and N. Imoto, *Phys. Rev. A* **64**, 063818 (2001).
 - [43] W. Leoński and R. Tanaś, *Phys. Rev. A* **49**, R20 (1994).
 - [44] A. Imamoglu, H. Schmidt, G. Woods, and M. Deutsch, *Phys. Rev. Lett.* **79**, 1467 (1997).
 - [45] W. Leoński and A. Kowalewska-Kudłaszyk (Elsevier, 2011) pp. 131 – 185.
 - [46] J. K. Kalaga, A. Kowalewska-Kudłaszyk, W. Leoński, and A. Barasiński, *Phys. Rev. A* **94**, 032304 (2016).
 - [47] S. Pandey, Z. Jiang, J. Combes, and C. M. Caves, *Phys. Rev. A* **88**, 033852 (2013).
 - [48] J. Bernu, S. Armstrong, T. Symul, T. C. Ralph, and P. K. Lam, *Journal of Physics B: Atomic, Molecular and Optical*

Physics **47**, 215503 (2014).

- [49] See Section III of Supplemental Material for the exact description with the proportionality constant.
- [50] See Section II of the Supplemental Material for details about the implementation and the associated success probability.
- [51] Obtained from (S49) of Supplemental Material for $\xi = 1$.
- [52] See Section III of the Supplemental Material for an iterative formula for the end-to-end heralded state and its RCI.
- [53] D. Gottesman, A. Kitaev, and J. Preskill, Phys. Rev. A **64**, 012310 (2001).
- [54] S. Pirandola, Communications Physics **2**, 51 (2019).
- [55] S. Pirandola, “Capacities of repeater-assisted quantum communications,” (2016), arXiv:1601.00966v4, 1601.00966.